**LETTER**

**Open Access**

CrossMark

# MEMS-based Ni–B probe with enhanced mechanical properties for fine pitch testing

Kyongtae Kim[†], Hong-Beom Kwon[†], Hye-Rin Ahn and Yong-Jun Kim[*]

## Abstract

We fabricated and characterized microelectromechanical systems (MEMS)-based Ni–B probes with enhanced mechanical properties for fine pitch testing. The Ni–B micro-probes were compared with conventional Ni–Co micro-probes in terms of the mechanical performance and thermal effect. The elastic modulus and hardness of Ni–B were found to be 240.4 and 10.9 GPa, respectively, which surpass those of Ni–Co. The Ni–B micro-probes had a higher contact force than the Ni–Co micro-probes by an average of 41.38% owing to the higher elastic modulus. The Ni–B micro-probes had a lower average permanent deformation than the Ni–Co micro-probes after the same overdrive was applied for 1 h by 56.58 μm. The temperature was found to have a negligible effect on the Ni–B micro-probes. These results show that Ni–B micro-probes are useful for fine pitch testing and a potential candidate for replacing conventional Ni–Co micro-probes owing to their advanced mechanical and thermal characteristics.

**Keywords:** Ni–B micro-probe, Ni–Co micro-probe, Contact force, Deformation

## Background

With the rapid growth in semiconductor technology for integrated circuit (IC) manufacturing processes, microelectromechanical systems (MEMS)-based probes play an important role in testing ICs on a wafer [1, 2]. The wafer-level test is the first step in the device manufacturing process, where chips fabricated on a bare wafer are subjected to standardized tests by using the input/output (I/O) terminals of the chips in order to determine defective chips before the packaging process [3]. During the wafer-level test, an individual chip is tested by using a probe card with micro-probes. This test makes it possible to reduce unnecessary packaging costs by avoiding the fabrication of defective devices at the initial stage. Because the test is conducted before the wafer is diced, it provides early feedback on the overall stages of the fabrication process so that corrections can be applied in an early stage of fabrication [4].

As the ICs on chips become more complex and the chip size becomes smaller, the number of test pads on the substrate increases, which has decreased the pitch among test pads. This trend requires narrower micro-probes, which in turn reduces the stiffness of the micro-probes. Micro-probes must exhibit high stiffness (or high elastic modulus if the geometry of the micro-probe is known) to be able to break the oxidation layer on aluminum I/O pads [4, 5]. In order to extend the service time, the mechanical properties of micro-probes should exhibit a high yield strength so that they do not undergo permanent deformation, high hardness to minimize the abrasion caused by a number of touchdowns, and high thermal stability so that they can maintain their mechanical performance in a high-temperature environment such as from localized Joule heating [5].

Under these conditions, Ni alloys, especially Ni–Co, are conventionally used for micro-probes because of their suitable properties and affordable fabrication processes, such as electroplating [2, 5–10]. However, since integration has increased continuously over the years, there is a growing need to find another material to meet the stringent requirements.

In this paper, we propose Ni–B as a potential candidate for micro-probes for fine pitch testing since it has been reported that alloying nickel with boron significantly enhances the hardness, elastic modulus, and creep

*Correspondence: yjk@yonsei.ac.kr
[†]Kyongtae Kim and Hong-Beom Kwon contributed equally to this work
School of Mechanical Engineering, Yonsei University, 50 Yonsei-ro, Seodaemun-gu, Seoul 120-749, Republic of Korea

Kim *et al. Micro and Nano Syst Lett (2017) 5:3*

Page 2 of 5

resistance [11, 12]. A MEMS Ni–B probe was fabricated by the electrodeposition technique. In order to measure the elastic modulus and hardness, we estimated the mechanical properties of electroplated Ni–B and Ni–Co by using nanoindentation. In addition, we conducted comparative experiments from various points of view to verify the applicability of Ni–B micro-probes to conventionally available Ni–Co micro-probes. The results showed that Ni–B micro-probes exhibit the potential applicability for micro-probes for fine-pitch testing.

## Design and fabrication

Figure 1 shows the proposed design of the micro-probes. The MEMS probes have a width of 50 μm. The geometry of the Ni–B micro-probes is identical to that of the Ni–Co micro-probes.

Here, 4-in silicon wafers were used as substrates, and a seed layer of Ti/Cu (50/500 nm) was deposited with electronic beam evaporation. The micro-probe patterns were fabricated by a photolithographic process using the photoresist THB-151N. The Ni–B probes were electroplated



**Fig. 1** Ni–B MEMS probes. **a** Proposed design and **b** fabricated probes

from a nickel sulfamate bath using dimethylamine borane (DMAB) as the B source. Then, the micro-probe patterns were removed by a stripper, and the Ni–B micro-probes were released by a 20% ammonium persulfate solution.

## Experimental details

In order to determine the hardness and elastic modulus of the micro-probes, nanoindentation tests were performed with a nanoindenter (G200, Agilent) having a Berkovich tip. The maximum load was 5 mN, and the loading and unloading rates were 1 mN/s. The Oliver–Pharr method was used to calculate the elastic modulus and hardness from the indentation load–displacement data.

The hardness of micro-probes, *H*, was estimated using

$$H = \frac{P_{max}}{A_c}, \tag{1}$$

where $P_{max}$ is the maximum load and $A_c$ is the projected contact area.

Elastic modulus, *E*, was estimated by its relationship with the projected contact area and the slope of an unloading curve at the beginning, which can be described as

$$E_{eff} = \frac{1}{2}\left(\frac{\pi}{A_c}\right)^{\frac{1}{2}} \frac{dP}{dh}\bigg|_{h=h_{max}}. \tag{2}$$

$E_{eff}$ is the effective elastic modulus and defined as

$$\frac{1}{E_{eff}} = \frac{1-v^2}{E} + \frac{(1-v_i)^2}{E_i}, \tag{3}$$

where $E_i = 1141$ GPa, $v_i = 0.07$ for Berkovich indenters, and $v = 0.3$ for micro-probes.

Figure 2a shows the MEMS probe testing system, which we developed in order to compare the performances of the Ni–B and Ni–Co micro-probes. The system consists of two parts: a control unit and measurement unit. The control unit is made up of a motion controller, stepping motor, stage, and motor driver. The measurement unit comprises a load cell and indicator. Figure 2b shows the setup of the system and a magnified photo of the stage with a micro-vice holding a probe.

We used the testing system to estimate the probes in terms of three properties, as listed in Table 1. We compared the performances of Ni–B and Ni–Co micro-probes fabricated with identical structures in terms of the contact force and deformation. The contact force was measured by using an electronic scale indicator with a load cell at increments of 25 μm overdrive (OD) from the contact point. After ODs (150, 300, 450 μm) were conducted for 1 h, the probes were captured, and the amount
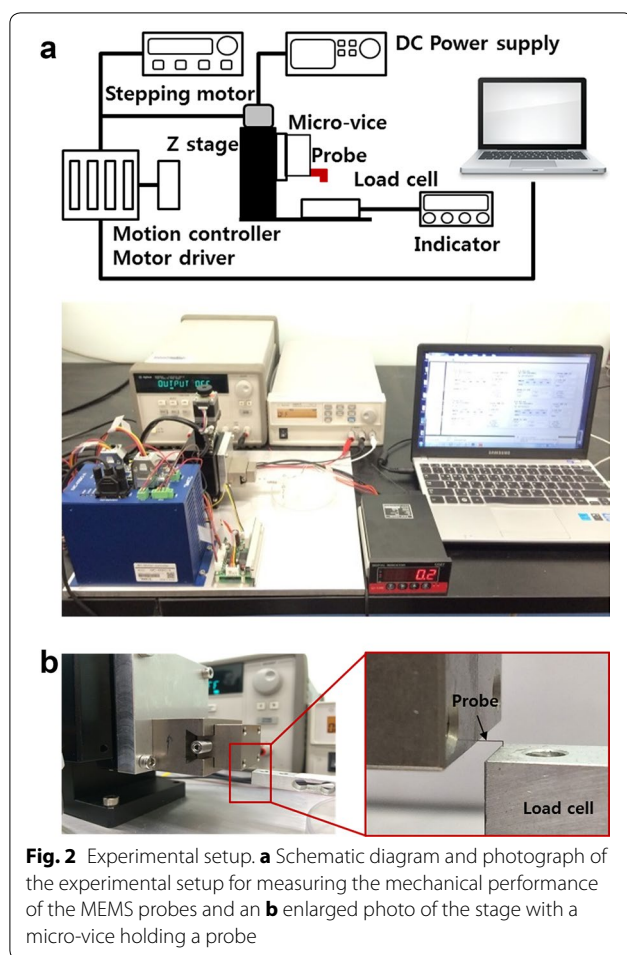
Kim *et al. Micro and Nano Syst Lett* (2017) 5:3

Page 3 of 5
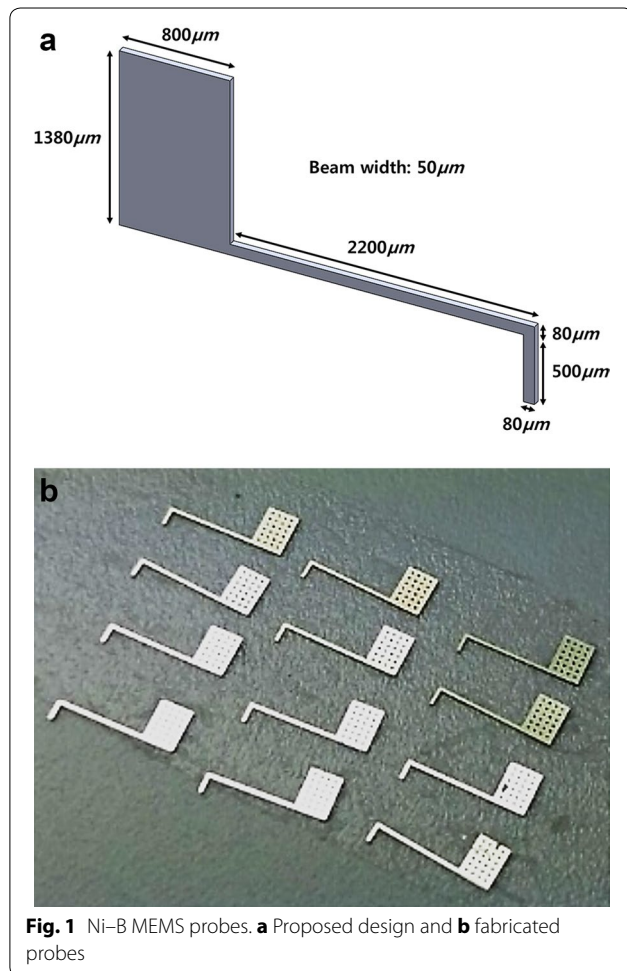


**Fig. 2** Experimental setup. **a** Schematic diagram and photograph of the experimental setup for measuring the mechanical performance of the MEMS probes and an **b** enlarged photo of the stage with a micro-vice holding a probe

**Table 1 Experimental conditions of Ni–B and Ni–Co MEMS probes**

| Test | Conditions |
|---|---|
| Contact force | Overdrive: 0–700 μm (25 μm) |
| Contact deflection | Overdrive: 150, 300, 450 μm<br>Time: 60 min/step |
| Thermal effect | Temperature: $23 \pm 5$, $95.5 \pm 5$ °C<br>Overdrive and time: same as above |

of deformation was evaluated with a microscope and its processor. The deformation was measured as the distance between the original point and the bent point of the probe beam. The thermal effect on Ni–B micro-probes was also evaluated. Under actual industrial conditions, electrical signal transmissions have a thermal effect on probes because of Joule heating. Thus, we estimated the stability of the Ni–B micro-probes by analyzing the contact forces and amount of deformation with the same method as described above at different temperatures: room temperature ($23 \pm 5$ °C) and high temperature ($95.5 \pm 5$ °C).

## Results and discussion

Figure 3 shows the load–displacement nanoindentation curves of Ni–B and Ni–Co and the corresponding hardness and elastic modulus. The hardness and elastic modulus of Ni–B were 10.9 and 240.4 GPa, respectively, which surpassed those of Ni–Co. This is because boron segregates into grains, and the grain boundaries impede dislocation transfer, which in turn hardens Ni–B.

Figure 4 shows the measured contact force as the OD was increased from 0 to 700 μm at room temperature. We tested the force five times and calculated the measurement average. The contact forces of the Ni–B micro-probes were greater than those of the Ni–Co micro-probes under every OD condition. The difference between the contact forces of the Ni–B and Ni–Co micro-probes increased with the amount of OD. This is because the elastic modulus of Ni–B that produced the reaction force was higher than that of Ni–Co, which is shown in the nanoindentation results. As shown in Fig. 4a, the contact force of the Ni–Co micro-probes hardly increased after an OD of more than about 250 μm, which indicates that the Ni–Co probe passed its yield point. On the other hand, the contact force of the Ni–B micro-probe still increased, which demonstrates that the Ni–B probe had a higher yield strength than the Ni–Co probe. The increasing ratio in Fig. 4b is determined by the contact force difference of Ni–B and Ni–Co micro-probes over the contact force of Ni–Co micro-probes; it can be expressed as follows:

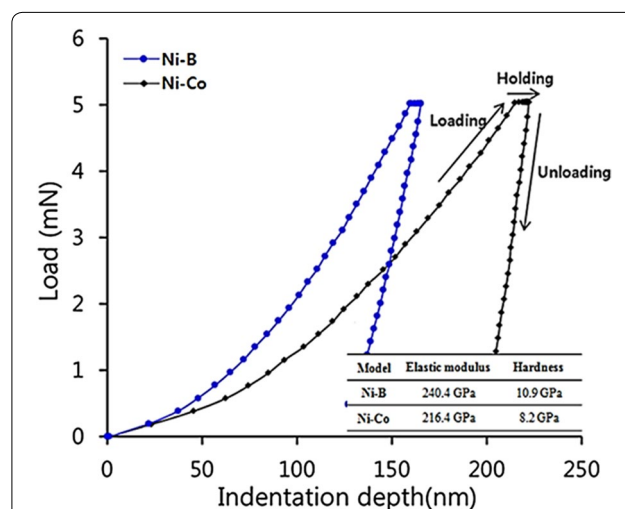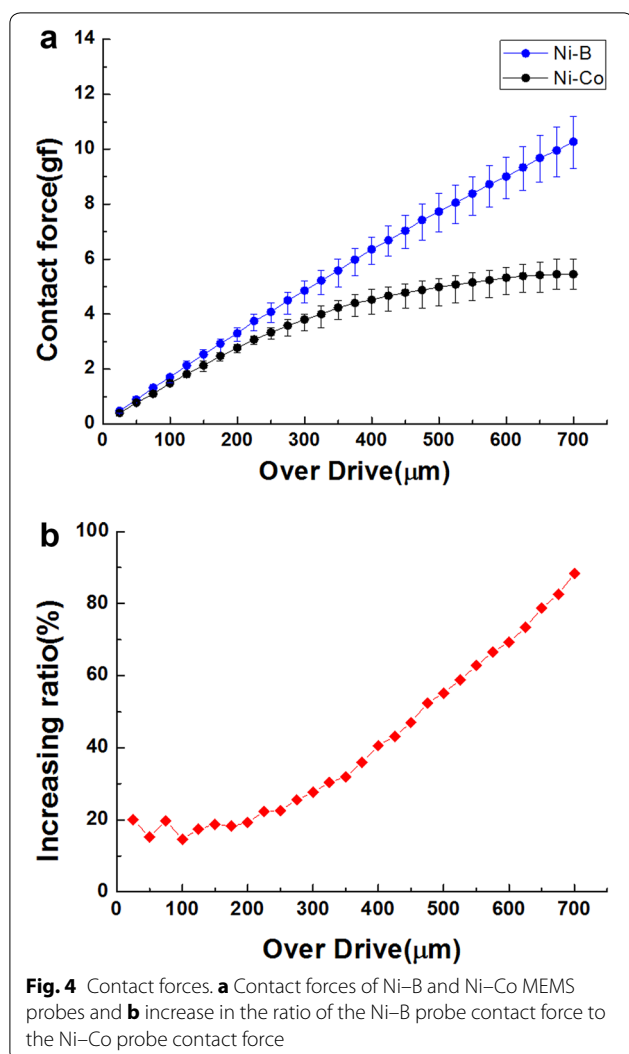$$Increasing\ ratio\ (\%) = \frac{F_{Ni-B} - F_{Ni-Co}}{F_{Ni-Co}} \times 100 \quad (4)$$



**Fig. 3** Load–displacement relationship. Load–displacement nanoindentation curves of Ni–B and Ni–Co and the resulting hardness and elastic modulus

Kim *et al. Micro and Nano Syst Lett* (2017) 5:3

Page 4 of 5



**Fig. 4** Contact forces. **a** Contact forces of Ni–B and Ni–Co MEMS probes and **b** increase in the ratio of the Ni–B probe contact force to the Ni–Co probe contact force



**Fig. 5** Permanent deformation. Permanent deformation of the Ni–B and Ni–Co MEMS probes when an overdrive was applied to each for 1 h

where $F_{Ni-B}$ is the Ni–B micro-probe contact force and $F_{Ni-Co}$ is the Ni–Co micro-probe contact force. The Ni–B micro-probe contact force increased by an average of 41.38% compared to that of Ni–Co along with the maximum increasing ratio of 88.38% and the minimum increasing ratio of 14.61% as shown in Fig. 4b. Based on these results, the Ni–B micro-probes should be able to break oxide layers on pads with enough contact force and manage to hold their structure without deformation over an extended testing period.

Next, we compared the resilience of the Ni–B and Ni–Co micro-probes by evaluating the amount of deformation from the contact deflection (Fig. 5). The deformation amount (λ) was measured as the displacement between the initial vertical length (a) and the deflected length (b). A comparative test was conducted with three different ODs: 150, 300, and 450 μm. Each OD was conducted for 1 h at room temperature. The difference in deformation increased with the OD, which is the same pattern as
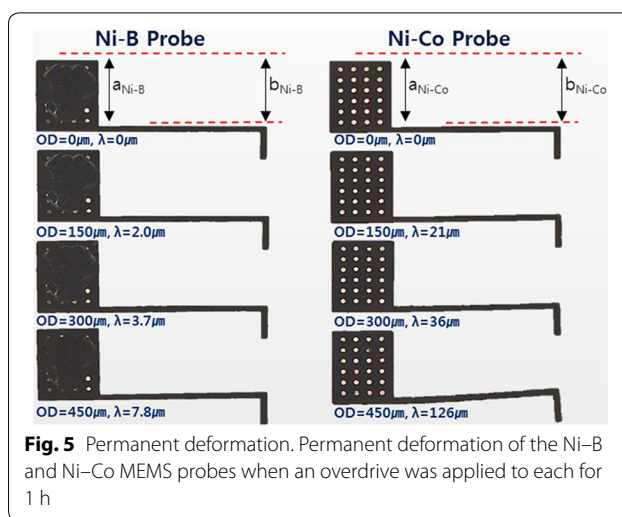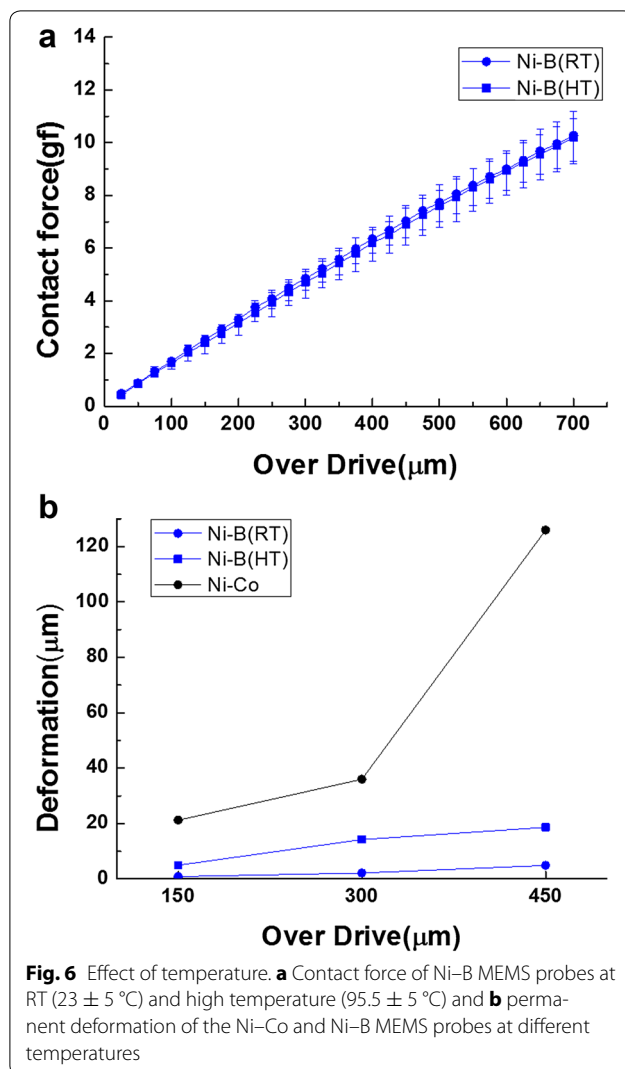
the contact force difference. The Ni–B probe deformed less than the Ni–Co probe by the average of 56.58 μm. The deformation of the Ni–Co probe was significantly affected with an OD of 450 μm, while the Ni–B probe maintained its level of deformation. We assumed that this is because Ni–B has a higher yield strength than Ni–Co. In addition, because the ODs were conducted for 1 h, the Ni–B micro-probes may be assumed to have a stronger creep resistance than the Ni–Co micro-probes.

Finally, the thermal stability of the Ni–B micro-probes was evaluated. Figure 6 shows the amount of contact force and permanent deformation as a function of OD at different temperatures (23 ± 5 and 95.5 ± 5 °C). As shown in Fig. 6a, the contact force behavior of Ni–Ni–BB probes did not changed at different temperatures, showing that the elastic modulus and yield point were not affected by their temperature change. Further, in Fig. 6b, the deformation results indicates that the Ni–B probes maintain their creep resistance at the high temperature and, in turn, prevent permanent deformation.

Overall, we confirmed that the Ni–B micro-probes managed to keep their mechanical properties not only at room temperature but also at the high temperature of 95.5 ± 5 °C.

## Conclusion
We presented Ni–B micro-probes with enhanced mechanical properties for fine pitch testing. We fabricated MEMS probes of Ni–B and Ni–Co with identical structures in order to compare their mechanical properties and prove the feasibility of Ni–B micro-probes. The hardness and elastic modulus of Ni–B and Ni–Co were measured by nanoindentation. Using our developed MEMS probe testing system, we tested the contact forces, deformation from the contact deflection, and

Kim *et al. Micro and Nano Syst Lett* (2017) 5:3

Page 5 of 5

**Fig. 6** Effect of temperature. **a** Contact force of Ni–B MEMS probes at RT (23 ± 5 °C) and high temperature (95.5 ± 5 °C) and **b** permanent deformation of the Ni–Co and Ni–B MEMS probes at different temperatures

thermal effect on the probes. All of the measurement and test results showed that the Ni–B micro-probe had superior mechanical properties. Based on these results, we concluded that the Ni–B micro-probes can sustain their mechanical performance for an extended service time and are useful for a large number of touchdown testing processes, which makes them potential replacements of conventional Ni–Co micro-probes for fine pitch testing.

**Abbreviations**
IC: integrated circuit; MEMS: microelectromechanical systems; I/O: input/output; OD: overdrive.

**References**
1. Wang F, Cheng R, Li X (2009) MEMS vertical probe cards with ultra densely arrayed metal probes for wafer-level IC testing. J Microelectromech Syst 18:933–941
2. Choi WC, Ryu JY (2012) Fabrication of a guide block for measuring a device with fine pitch area-arrayed solder bumps. Microsyst Technol 18:333–339
3. Kim BH, Kim HC, Choi SD, Chun K, Kim JB, Kim JH (2007) A robust MEMS probe card with vertical guide for a fine pitch test. J Micromech Microeng 17:1350–1359
4. Yuan T, Chen D, Chen J, Fu H, Kurth S, Otto T, Gessner T (2013) Design, fabrication and characterization of MEMS probe card for fine pitch IC testing. Sens Actuators A Phys 204:67–73
5. Kim BH, Kim JB (2009) Design and fabrication of a highly manufacturable MEMS probe card for high speed testing. J Micromech Microeng 18:075031
6. Kim BH, Park BJ, Kim JB (2009) Process effects of double step DRIE and Ni–Co electroplating for a trench-type cantilever probe for a fine-pitched MEMS probe card. Sens Actuators A Phys 152:252–260
7. Lee KY, Huang JT, Chao PS, Lin JM, Hsu HJ (2014) An integrated electroless nickel plating process for fabrication of CMOS-MEMS probe chip. Microelectron Eng 113:147–151
8. Kim BH, Cho C, Lee B, Kim HC, Chun K (2012) Design and fabrication of microelectromechanical systems probe card with vertical trench guide for fine pitch probing. J Appl Phys 51:06FL16
9. Kim JH, Chu SI, Seo HW, Ryu JW, Kim GT, Moon S (2007) Fabrication and characteristics of MEMS vertical type probe tip for micro sized pads measurement. In: 20th International conference on micro electro mechanical systems. IEEE, Hyogo, 21–25 Jan 2007, pp 283–286
10. Namazu T, Inoue S, Tashiro Y, Okamura Y, Koterazawa K (2005) Ti–Ni SMA film actuated Si cantilever beams for MEMS probe card. In: The 13th International conference on solid-state sensors, actuators and microsystems. IEEE, Seoul, 5–9 June 2005, vol 1, pp 733–736
11. Yin WM, Whang SH, Mirshams RA (2005) Effect of interstitials on tensile strength and creep in nanostructured Ni. Acta Mater 53:383–392
12. Domínguez-Ríos C, Hurtado-Macias A, Torres-Sánchez R, Ramos MA, González-Hernández J (2012) Measurement of mechanical properties of an electroless Ni–B coating using nanoindentation. I&EC Res 51:7762–7768